



RESEARCH LETTER

10.1002/2017GL076116

Key Points:

- Uncertainty in sea level projections is a major challenge to community level adaptation
- The proposed approach helps translating complex datasets with scientific uncertainty to communicable information
- The output of the process is the probability distribution of road network flooding conditioned on emission scenarios

Correspondence to:

A. AghaKouchak,
amir.a@uci.edu

Citation:

Moftakhari, H., AghaKouchak, A., Sanders, B. F., Matthew, R. A., & Mazdiyasn, O. (2017). Translating uncertain sea level projections into infrastructure impacts using a Bayesian framework. *Geophysical Research Letters*, 44, 11,914–11,921. <https://doi.org/10.1002/2017GL076116>

Received 19 OCT 2017

Accepted 9 NOV 2017

Accepted article online 13 NOV 2017

Published online 11 DEC 2017

Translating Uncertain Sea Level Projections Into Infrastructure Impacts Using a Bayesian Framework

Hamed Moftehkhari¹ , Amir AghaKouchak^{1,2} , Brett F. Sanders^{1,3}, Richard A. Matthew^{3,4}, and Omid Mazdiyasn¹

¹Department of Civil and Environmental Engineering, University of California, Irvine, CA, USA, ²Department of Earth System Science, University of California, Irvine, CA, USA, ³Department of Urban Planning and Public Policy, University of California, Irvine, CA, USA, ⁴Blum Center for Poverty Alleviation, University of California, Irvine, CA, USA

Abstract Climate change may affect ocean-driven coastal flooding regimes by both raising the mean sea level (msl) and altering ocean-atmosphere interactions. For reliable projections of coastal flood risk, information provided by different climate models must be considered in addition to associated uncertainties. In this paper, we propose a framework to project future coastal water levels and quantify the resulting flooding hazard to infrastructure. We use Bayesian Model Averaging to generate a weighted ensemble of storm surge predictions from eight climate models for two coastal counties in California. The resulting ensembles combined with msl projections, and predicted astronomical tides are then used to quantify changes in the likelihood of road flooding under representative concentration pathways 4.5 and 8.5 in the near-future (1998–2063) and mid-future (2018–2083). The results show that road flooding rates will be significantly higher in the near-future and mid-future compared to the recent past (1950–2015) if adaptation measures are not implemented.

1. Introduction

Climate model projections of future sea levels are critical to community level adaptation, defined as a set of strategies and actions with the aim of moderating harm or exploiting beneficial opportunities (Moser & Ekstrom, 2010; Pielke et al., 2007). Sea level rise represents a major threat to coastal ecosystems (Epanchin-Niell et al., 2017; Webb et al., 2013) and development (Field et al., 2014; Hallegatte et al., 2013; Hanson et al., 2011; Nicholls et al., 2008), and adaptation to sea level rise calls for climate model projections that go beyond mean sea level and include variability (Dangendorf et al., 2017). For example, extreme high water level distributions are critical to the assessment of flooding hazards (Arns et al., 2017; Muis et al., 2017), and coastal habitats such as tidal marshes are sensitive to inundation regimes resulting from the occurrence of both low and high water levels (Scavia et al., 2002; Temmerman et al., 2013). A general approach to predict future variability in regional sea states from climate models focuses on prediction of total water level (TWL),

$$TWL = T + msl + NTR \quad (1)$$

where T represents the astronomical tide height, msl represents the mean sea level, and NTR represents the nontidal residual in sea level which captures the effects of storm surges, trapped coastal waves, interannual phenomena such as El Niño, and other processes that contribute to differences from the astronomical tide height (Barnard et al., 2015; Ruggiero, 2013; Serafin et al., 2017). TWL usually omits variability in sea levels due to waves (i.e., time scales of seconds). Additionally, TWL as defined in equation (1) represents an absolute height relative to a fixed geodetic datum, assuming msl is also defined relative to a fixed datum. Relative water levels that account for land subsidence are thus obtained by adding the rate of land subsidence to equation (1) (Kopp et al., 2014; Pfeffer & Allemand, 2016).

Applications of equation (1) to predict future TWL typically assume that T is a harmonic function with tidal constituents that do not vary over time. The estimates of change in msl between the present and future time of interest, referred to as sea level rise (SLR), are taken from one or more climate models (Carson et al., 2016; Kopp et al., 2014), and NTR is treated as a stochastic process that is either modeled based on historical tide data or predicted by advanced climate models that resolve nontidal sea level variability at fine temporal scales (Cayan et al., 2008; Serafin & Ruggiero, 2014). Hence, TWL represents a stochastic process with several sources of uncertainty including uncertainty in T (Leffler & Jay, 2009), uncertainty in SLR

(Buchanan et al., 2016), and uncertainty in NTR (Cayan et al., 2008). Uncertainties can be further divided into various types: emission scenario uncertainty (e.g., RCP 4.5 versus RCP 8.5), climate model structure uncertainty, and downscaling uncertainty (Eghdamirad et al., 2016; Kopp et al., 2014; Najafi et al., 2011; O'Neill et al., 2017). Efforts to project future sea levels have thus resulted in large data sets designed to capture uncertainty from many different sources. Here we analyze the outputs from eight different climate models, two different emission scenarios (RCPS 4.5 and 8.5), and two different percentiles (50th and 95th)—a total of 32 different sets of model outputs for sites along the California coast (details in section 2). This poses a major challenge to community level adaptation: translating large and complex data sets with scientific uncertainty to diverse end-users of information within affected communities (Di Baldassarre et al., 2016; Faulkner et al., 2007; Wahl et al., 2017). While dealing with significant uncertainties is one important dimension of the challenge, another challenge is effective communication with decision points within affected communities (Adger et al., 2009; Buchecker et al., 2013; Nyborg et al., 2016; Spiekermann et al., 2015).

In this study, we present an approach to synthesize TWL projections with uncertainty around a targeted impact of concern within a community. Here this impact is chosen as the exposure of regional road networks to flooding measured in kmh/yr. Our approach leverages the availability of local tide data to weigh output from available climate models in a systematic way, and ultimately produces a limited set of exposure projections conditioned only on emission scenarios and chosen percentiles. That is, the output of the process is the probability distribution of road network flooding conditioned on emission scenarios.

Roadway flooding is the targeted impact of concern for several reasons. First, transportation is a key driver of economies (Eddington, 2006), and interruptions in service can have disastrous outcomes (Asadabadi & Miller-Hooks, 2017; Jaroszweski et al., 2010; United Nations, 2013). Second, many transportation networks are already exposed to flooding, and the potential exists for major increases in exposure with SLR (Kulp & Strauss, 2017; Titus, 2002). Third, repair and replacement of transportation infrastructure is costly, and increased flooding threatens shorter service life which increases lifecycle costs (Barnes et al., 2017; Rattanachot et al., 2015).

2. Data

The approach presented here to synthesize sea level projections with infrastructure impacts relies on three key data sets: (i) Projections of hourly TWL (including T , msl, and NTR) for the multidecadal period of interest (e.g., 1950–2100), (ii) exposure data that tabulates infrastructure impacts (in this case roadway km exposed to flooding) versus TWL, and (iii) historical TWL data over a portion of the multidecadal period of interest (e.g., 1950–2015).

Observed hourly TWL data at tide gauges located in San Francisco (NOAA ID 9414290) and Los Angeles (NOAA ID 9410660) between years 1950 and 2015 are provided by the National Oceanic and Atmospheric Association (NOAA: <https://tidesandcurrents.noaa.gov>). The records for these two gauges are fairly complete with gaps of less than 1% over the length of record. Predictions for the tide (T) based on harmonic analysis of the tidal constituents is also provided for both sites, and we calculate the historic surge (NTR) activity by taking the difference between observed (TWL) and the predicted ($T + \text{msl}$) values.

Future sea level projections provided by *Scripps Institution of Oceanography* consist of all three components of TWL (Cayan et al., 2008). The methodology and data used for mean SLR projections under different future representative concentration pathways (RCP) 4.5 and 8.5 are explained in Cayan et al. (2016). The SLR projections are presented in percentiles to enable users to quantify the uncertainties associated with these estimates. In this work we use 50th and 95th percentiles of the projected SLR. The tides are predicted based on the harmonic constituents estimated by NOAA. For the surge component (NTR), eight global climate models (GCMs) are selected based on the recommendations of Climate Change Technical Advisory Group (CCTAG) of California Department of Water Resources. Out of 10 GCMs that CCTAG determined to be the most representative of California climate, the downscaled (a grid with $0.25^\circ \times 0.25^\circ$ spatial resolution) and bias-corrected winds and pressures from eight GCMs (listed in Table 1) are used. These eight GCMs contain all daily variables needed to estimate the hourly sea level projections between 1950 and 2100.

The lengths of the unprotected (i.e., connected to the ocean) roads below sea level for any given incident water level exceedance above mean higher high water (MHHW; the average of the higher high water

Table 1
Calculated Weights

Model		ACCESS1-0	CanESM2	CMCC-CMS	CNRM-CM5	GFDL-CM3	HadGEM2-CC	HadGEM2-ES	MIROC5
Los Angeles	Weights	0.1368	0.1338	0.1378	0.1420	0.0290	0.1401	0.1480	0.1323
	Sigma square	0.0028	0.0022	0.0026	0.0025	0.4060	0.0025	0.0024	0.0025
San Francisco	Weights	0.1273	0.1287	0.1261	0.1261	0.1179	0.1252	0.1307	0.1179
	Sigma square	0.0096	0.0064	0.0044	0.0060	0.0081	0.0046	0.0059	0.0081

height of each tidal day observed over the National Tidal Datum Epoch) for Orange County and Marin County, California, USA are obtained from the risk finder tool provided by Climate Central (<http://sealevel.climatecentral.org/>) (Kulp & Strauss, 2017; Tebaldi et al., 2012). These counties are selected based on their vulnerability to coastal road flooding. Orange County (with 2,000 km² land area) has ~350 km of roads below coastal water level with 1 m of SLR above MHHW, 71 km of which connected to the ocean (not protected with levees). Coastal flooding in Marin County (with 1,300 km² land area) is an emerging issue (BVB Consulting, 2017), too, with 180 km of roads below coastal water level with 1 m of rise above MHHW, 148 km of which connected to the ocean.

3. Methods

3.1. Exposure Estimation

Following Moftakhari et al. (2017), we estimate the expected lengths of roads exposed to coastal flooding (E) associated with each TWL incidence above MHHW (Z) via

$$E_{(Z)} = L_{(Z)} \times P_{(Z)}, \tag{2}$$

where $L_{(Z)}$ is the lengths of roads inundated at any flood incidence and $P_{(Z)}$ represents the likelihood of TWL exceedance above MHHW for the analyzed tide gauges. $P_{(Z)}$ is empirically calculated for the studied time windows. For the near-future and mid-future projections, $P_{(Z)}$ is calculated over a time window with the same length of historic window (i.e., 65 years) and centered around the projection year (e.g., 2030 and 2050).

The road exposure data from Climate Central is provided for 10 different SLR values (i.e., 0.3–3 m above MHHW). Thus, for the purpose of this work we need to interpolate between exposure estimates (Figure 1). A single nonlinear curve of the form

$$L_{(Z)} = \alpha + \beta Z^\gamma \tag{3}$$

is a good approximation road exposure $L_{(Z)}$ as a function of TWL above MHHW (Z) for $Z > 0.61$ m, where α , β , and γ are parameters to be calibrated through nonlinear regression analysis. However, the fitted nonlinear curve poorly represents the road exposure for Z less than 2 ft (~0.61 m above MHHW). Hence, exposure estimates associated with $Z \leq 0.61$ m (Figure 1) are linearly interpolated.

3.2. Ensemble Generation

At each gauge the storm surge for a given RCP is predicted based on the outputs of eight different GCMs. We have used Bayesian Model Averaging (BMA) to produce a weighted ensemble of the modeled surges so we can quantify the likelihood of flooding under each scenario. BMA is a well-known averaging methodology that combines the forecast densities of multiple models to produce a new forecast probability density function (Najafi & Moradkhani, 2016). The predictive distribution of a forecast variable y , given independent predictions of n models $[M_1, M_2, \dots, M_n]$ (here eight GCMs), and observations during training period Y (here 1950–2015) can be expressed as

$$p(y|M_1, M_2, \dots, M_n, Y) = \sum_{i=1}^n p(M_i|Y)p(y|M_i, Y), \tag{4}$$

where $p(y|M_i, Y)$ is the posterior distribution of y given the model prediction M_i , and the training data Y . In other words, $p(y|M_i, Y)$ is the forecast probability density function of y , given model i , and $p(M_i|Y)$ is the likelihood that the model prediction is correct, given Y (the observations) during the training period. To meet the BMA assumptions, all the storm surge values were transformed using the Box-Cox transformation to ensure that the probability distribution of the prediction errors follows the Gaussian distribution. The likelihood (aka weight) estimates are obtained from application of the Expectation Maximization procedure (Duan et al.,

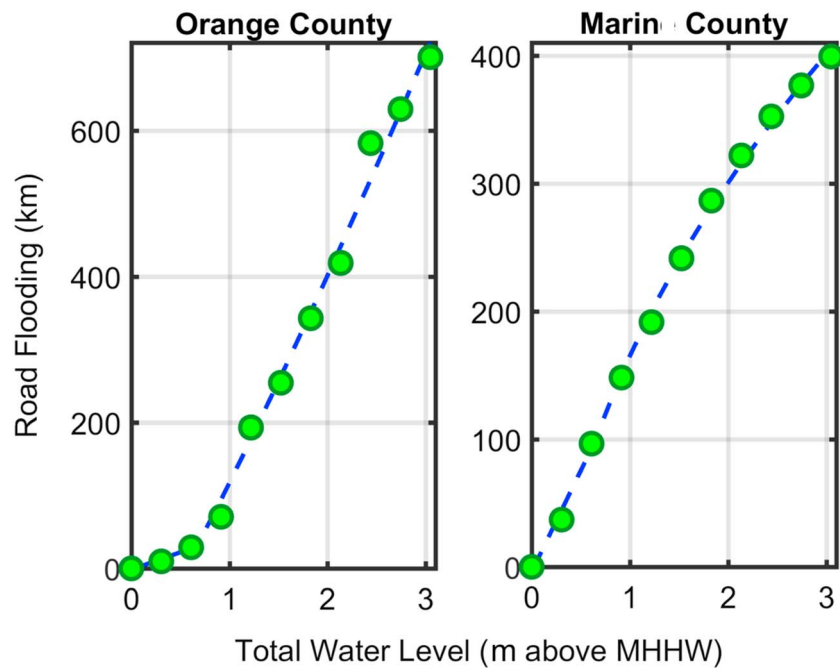


Figure 1. Length of roads exposed to coastal flooding under the incident rise of total water above mean higher high water (MHHW).

2007). These weights reflect the performance of each GCM in reproducing the historic surge patterns and are provided in Table 1. Then, the resulting probability density functions are used to quantify the change in frequency of road flooding in the future, relative to the past. For further details regarding the BMA and the model used in this work, see Madadgar and Moradkhani (2014), Najafi et al. (2011), and Najafi and Moradkhani (2015, 2016).

4. Results and Discussions

Figure 2 shows the cumulative distribution function (CDF) of observed, historic model simulation and projected water levels in Los Angeles and San Francisco as follows: (i) the thick brown line represents observed hourly water level from 1950 to 2015, (ii) the thin green line represents simulated hourly water level from BMA for 1950–2015, (iii) the solid black line represents the projected water level given the 50th percentile of projected mean sea level (msl) under climate scenario RCP 4.5, (iv) the dashed black line represents the water level given the 95th percentile of the projected msl under climate scenario RCP 4.5, (v) the solid red line represents the estimated water level given the 50th percentile of projected msl under climate scenario RCP 8.5, and (vi) the dashed red line represents the resulting water level given the 95th percentile of the projected msl and under climate scenario RCP 8.5. At Los Angeles, both observed water level and the BMA simulation indicate that the likelihood (i.e., $1 - \text{CDF}$) of TWL exceeding MHHW (dashed blue line) is approximately 5% over the period 1950–2015. However, in near-future (1998–2063), the likelihood that TWL exceeds MHHW rises up to 6% and 8% under the projected 50th and 95th percentiles of SLR, respectively. This likelihood is even higher under projections for mid-future (2018–2083), ranging between 9% (RCP 4.5, 50th SLR percentile) and 17% (RCP 8.5, 95th SLR percentile). San Francisco is expected to experience more TWL exceeding MHHW in the mid-future to near-future, relative to the past with likelihood of 3%. In near-future this likelihood is 5% and 7% under the projected 50th and 95th percentiles of SLR, respectively. Further increase is revealed for mid-future in which the likelihood is significantly higher and ranges between 11% (RCP 4.5, 50th SLR percentile) and 19% (RCP 8.5, 95th SLR percentile). This substantial increase in the probability of coastal water level exceeding MHHW can have significant impacts on coastal infrastructure.

Figure 3 shows how change in the likelihood that TWL exceeds a given threshold (here MHHW) contributes to increased risk of flooding. In Orange County under the historic TWL simulated at Los Angeles between 1950 and 2015, we currently expect to experience ~35,800 kilometer hour (kmh) of road flooding. This

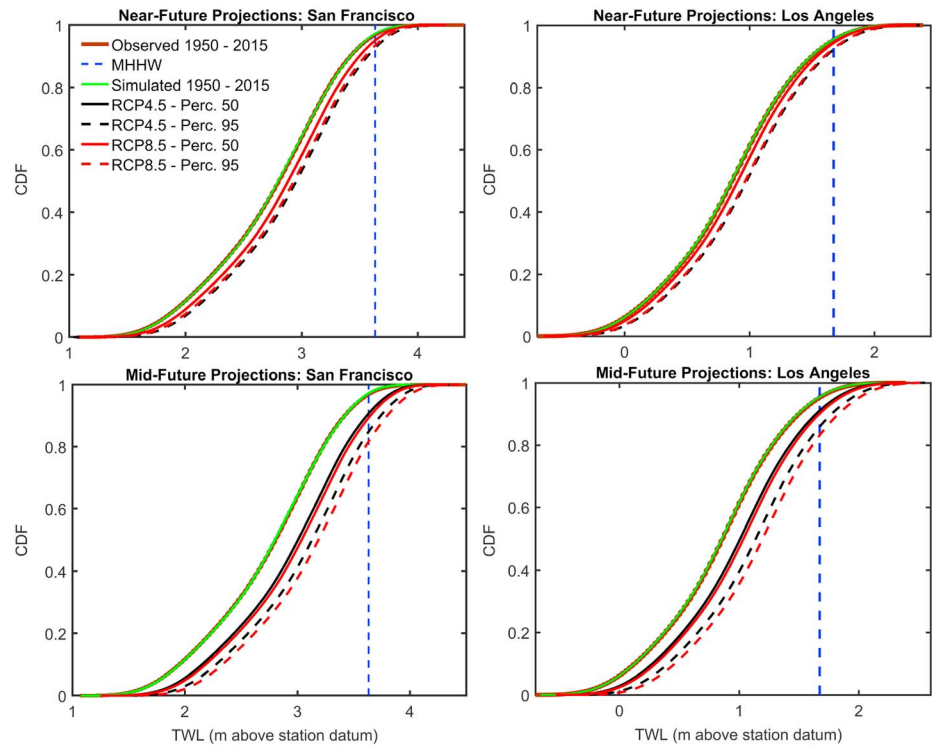


Figure 2. Cumulative distribution function of total water level above the station datum for the historical (1950–2015) observation/simulations and future projections in near future (1998–2063) and midfuture (2018–2083). For the future projections the curve shows the estimated CDF under the underlying RCP scenarios and the given percentiles of mean sea level rise.

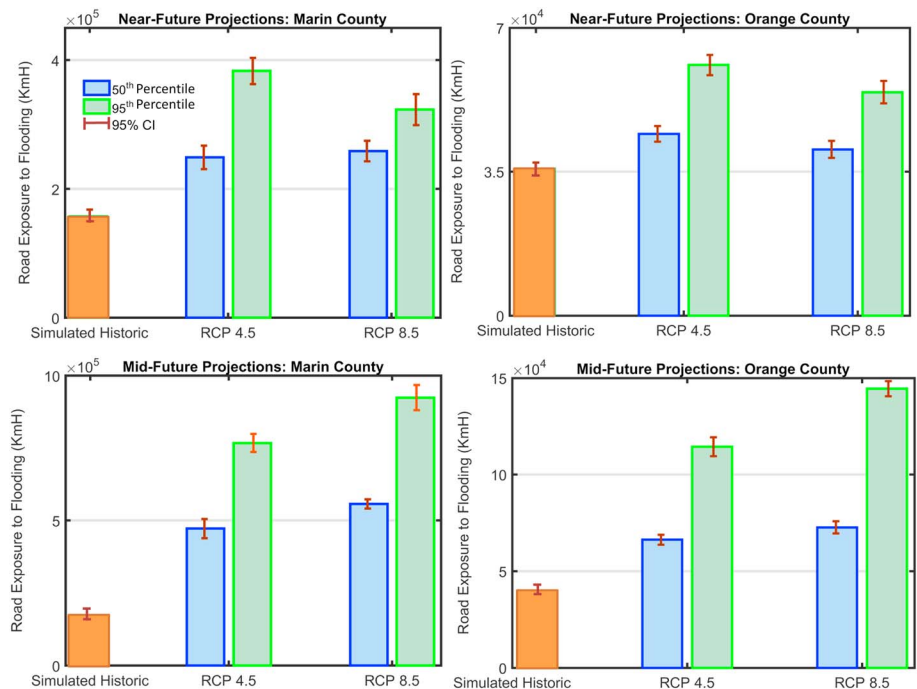


Figure 3. Estimated road exposure to flooding for simulated historic coastal ocean water dynamics and under the future RCP scenarios and the given percentiles of mean sea level rise.

number, which is already significant and costly (Moftakhari et al., 2017), will rise in near-future (between 40,000 and 61,000 kmh) and mid-future (between 67,000 and 145,000 kmh), if no mitigation measures are implemented. These numbers are based on a weighted ensemble of TWL from BMA, and error bars in this figure show the 95% confidence limits. Marin County is currently expected to experience ~160,000 kmh of road flooding in a given year, due to the TWL regime simulated at tide gauge in San Francisco, but will experience higher rates in the following decades. As shown in Figure 3, Marin County should expect road flooding of between 250,000 and 380,000 kmh in near future, which is roughly 1.5 to 2.5 times higher than present. Without adaptation, road flooding could reach ~3 to 6 higher values (470,000 and 925,000 kmh) in midfuture.

In near-future, a higher rate of flooding is expected under RCP 4.5 compared with RCP 8.5 (Figures 3a and 3b). This can be attributed to either different short-term rising patterns in mean sea level, lower frequency/intensity of storm surges under RCP 8.5, or both. In near-term, internal variability (Bromirski et al., 2011) due to a combination of dynamic and static equilibrium effects (Hay et al., 2013; Kopp et al., 2010) would significantly affect the estimation of local sea level changes (Kopp et al., 2014). Also, the frequency and intensity of storm events are expected to be altered in northeastern Pacific Ocean under a changing climate (Shope et al., 2016). For example, significant wave height is expected to decrease south of ~50°N. This decrease is projected to be larger under RCP 8.5 compared to RCP 4.5 (Erikson et al., 2015).

The results of this study are based on two major assumptions. First, the rates of exposure estimated in this study include only the roads that are connected to the ocean and exclude those sheltered by flood defences (i.e., levees). So we have assumed that flood defences do not fail during future flood events. In case of a failure these rates could be considerably higher. A second assumption underlying the estimates provided here is that no adaptation measure takes place over the given time horizon. In other words, the model used here assumes that the parameters describing the road inundation for any incidence above MHHW (i.e., the curve in Figure 1) are stationary and do not change over time. Obviously, any suite of interventions that avoid or minimize the impacts of coastal flooding hazards on vulnerable systems (here roads exposed to ocean water) and makes the threatened community less prone to the adverse effects of a flood hazard, referred to as adaptation (Jongman et al., 2015; Schipper, 2009), should be included in decision making and risk assessment practices.

Effective risk communication, defined as purposeful exchange of information about risks between interested parties (Covello et al., 1986), with the aim of aiding decision makers to raise risk preparedness (Kellens et al., 2013; Maidl & Buchecker, 2015) requires a translational discourse between scientists and professionals in risk management (Faulkner et al., 2007). The approach presented here is not a substitute for such discourse but rather constitutes a tool to enhance discourse through the transformation of complex data sets into relatively simple and targeted metrics that facilitates risk communication (Weaver et al., 2017).

Acknowledgments

Financial support for this study was provided by the National Science Foundation Hazards-SEES Program (award DMS 1331611) and the National Oceanic and Atmospheric Administration Ecological Effects of Sea Level Rise Program (award NA16NOS4780206). We also acknowledge California's Fourth Climate Change Assessment model simulations and California Energy Commission award 500-15-005. The data for road lengths exposed to flooding under different sea level rise scenarios are obtained from the risk finder tool provided by Climate Central (<http://sealevel.climatecentral.org/>). The hourly water level data for all tide gauges are provided by National Oceanic and Atmospheric Association (NOAA; <http://tidesandcurrents.noaa.gov/>). We also thank Daniel Cayan, David Pierce, and Julie Kalansky from Scripps Institution of Oceanography, University of California, San Diego, for providing hourly sea level projections at the studied tide gauges.

5. Conclusions

A general approach utilizing BMA is presented to combine surge predictions (NTRs) from different climate models with tidal predictions and sea level rise projections to statistically characterize the distribution of roadway coastal flooding. BMA performs well in reproducing historic NTRs (Figure 2) with relatively small errors in estimated weights (Table 1). The results suggest that sea level rise and change in storm surge patterns will increase road flooding exposures to both Orange County and Marin County 2–4 times and 3–6 times higher, in near-future and mid-future, respectively, if no adaptation measure takes place. Furthermore, the BMA approach presented here poses an opportunity to simplify public communication about the likelihood of flooding under climate change without sacrificing scientific depth, based on a systematic approach of combining climate model output and uncertainty. The proposed approach is applicable to any type of infrastructure where impacts scale with water levels.

References

- Adger, W. N., Dessai, S., Goulden, M., Hulme, M., Lorenzoni, I., Nelson, D. R., ... Wreford, A. (2009). Are there social limits to adaptation to climate change? *Climatic Change*, 93(3–4), 335–354. <https://doi.org/10.1007/s10584-008-9520-z>
- Arns, A., Dangendorf, S., Jensen, J., Talke, S., Bender, J., & Pattiaratchi, C. (2017). Sea-level rise induced amplification of coastal protection design heights. *Scientific Reports*, 7, 40171. <https://doi.org/10.1038/srep40171>

- Asadabadi, A., & Miller-Hooks, E. (2017). Optimal transportation and shoreline infrastructure investment planning under a stochastic climate future. *Transportation Research Part B: Methodological*, *100*, 156–174. <https://doi.org/10.1016/j.trb.2016.12.023>
- Barnard, P. L., Short, A. D., Harley, M. D., Splinter, K. D., Vitousek, S., Turner, I. L., ... Heathfield, D. K. (2015). Coastal vulnerability across the Pacific dominated by El Niño/Southern Oscillation. *Nature Geoscience*, *8*(10), 801–807. <https://doi.org/10.1038/ngeo2539>
- Barnes, S. R., Bond, C., Burger, N., Anania, K., Strong, A., Weiland, S., & Virgets, S. (2017). Economic evaluation of coastal land loss in Louisiana. *Journal of Ocean and Coastal Economics*, *4*(1). <https://doi.org/10.15351/2373-8456.1062>
- Bromirski, P. D., Miller, A. J., Flick, R. E., & Auad, G. (2011). Dynamical suppression of sea level rise along the Pacific coast of North America: Indications for imminent acceleration. *Journal of Geophysical Research*, *116*, C07005. <https://doi.org/10.1029/2010JC006759>
- Buchanan, M. K., Kopp, R. E., Oppenheimer, M., & Tebaldi, C. (2016). Allowances for evolving coastal flood risk under uncertain local sea-level rise. *Climatic Change*, *137*(3–4), 347–362. <https://doi.org/10.1007/s10584-016-1664-7>
- Buchecker, M., Salvini, G., Di Baldassarre, G., Semenzin, E., Maidl, E., & Marcomini, A. (2013). The role of risk perception in making flood risk management more effective. *Natural Hazards and Earth System Sciences*, *13*(11), 3013–3030. <https://doi.org/10.5194/nhess-13-3013-2013>
- BVB Consulting (2017). Marin shoreline sea level rise vulnerability assessment. Marin County Department of Public Works. Retrieved from https://www.marincounty.org/~media/files/departments/cd/slr/baywave-va/public_review_draft_baywave_marinshorelinevulnerability-assessment_s.pdf?la=en
- Carson, M., Köhl, A., Stammer, D., Slangen, A., Katsman, C., van de Wal, R., ... White, N. (2016). Coastal sea level changes, observed and projected during the 20th and 21st century. *Climatic Change*, *134*(1–2), 269–281. <https://doi.org/10.1007/s10584-015-1520-1>
- Cayan, D. R., Bromirski, P. D., Hayhoe, K., Tyree, M., Dettinger, M. D., & Flick, R. E. (2008). Climate change projections of sea level extremes along the California coast. *Climatic Change*, *87*(S1), 57–73. <https://doi.org/10.1007/s10584-007-9376-7>
- Cayan, D. R., Kalansky, J., Icobellis, S., & Pierce, D. (2016). *Creating probabilistic sea level rise projections (climate adaptation and resiliency no. 16-IEPR-04)*. La Jolla, CA: California Energy Commission.
- Covello, V., von Winterfeldt, D., & Slovic, P. (1986). Risk communication: A review of literature. *Risk Abstracts*, *3*, 171–182.
- Dangendorf, S., Marcos, M., Wöppelmann, G., Conrad, C. P., Frederikse, T., & Riva, R. (2017). Reassessment of 20th century global mean sea level rise. *Proceedings of the National Academy of Sciences*, *114*(23), 5946–5951. <https://doi.org/10.1073/pnas.1616007114>
- Di Baldassarre, G., Brandimarte, L., & Beven, K. (2016). The seventh facet of uncertainty: Wrong assumptions, unknowns and surprises in the dynamics of human–water systems. *Hydrological Sciences Journal*, *61*(9), 1748–1758. <https://doi.org/10.1080/02626667.2015.1091460>
- Duan, Q., Ajami, N. K., Gao, X., & Sorooshian, S. (2007). Multi-model ensemble hydrologic prediction using Bayesian model averaging. *Advances in Water Resources*, *30*(5), 1371–1386. <https://doi.org/10.1016/j.advwatres.2006.11.014>
- Eddington, R. (2006). *The Eddington transport study: Main report: Transport's role in sustaining the UK's productivity and competitiveness*. Norwich: TSO.
- Eghdamirad, S., Johnson, F., Woldemeskel, F., & Sharma, A. (2016). Quantifying the sources of uncertainty in upper air climate variables: Uncertainty in atmospheric variables. *Journal of Geophysical Research: Atmospheres*, *121*, 3859–3874. <https://doi.org/10.1002/2015JD024341>
- Epanchin-Niell, R., Kousky, C., Thompson, A., & Walls, M. (2017). Threatened protection: Sea level rise and coastal protected lands of the eastern United States. *Ocean and Coastal Management*, *137*, 118–130. <https://doi.org/10.1016/j.ocecoaman.2016.12.014>
- Erikson, L. H., Hegermiller, C. A., Barnard, P. L., Ruggiero, P., & van Ormondt, M. (2015). Projected wave conditions in the Eastern North Pacific under the influence of two CMIP5 climate scenarios. *Ocean Modelling*, *96*, 171–185. <https://doi.org/10.1016/j.ocemod.2015.07.004>
- Faulkner, H., Parker, D., Green, C., & Beven, K. (2007). Developing a translational discourse to communicate uncertainty in flood risk between science and the practitioner. *Ambio: A Journal of the Human Environment*, *36*(8), 692–704. [https://doi.org/10.1579/0044-7447\(2007\)36%5B692:DATDTC%5D2.0.CO;2](https://doi.org/10.1579/0044-7447(2007)36%5B692:DATDTC%5D2.0.CO;2)
- Field, C. B., Barros, V. R., & Intergovernmental Panel on Climate Change (Eds.) (2014). *Climate change 2014: Impacts, adaptation, and vulnerability: Working Group II contribution to the fifth assessment report of the Intergovernmental Panel on Climate Change*. New York, NY: Cambridge University Press. <https://doi.org/10.1017/CBO9781107415379>
- Hallegratte, S., Green, C., Nicholls, R. J., & Corfee-Morlot, J. (2013). Future flood losses in major coastal cities. *Nature Climate Change*, *3*(9), 802–806. <https://doi.org/10.1038/nclimate1979>
- Hanson, S., Nicholls, R., Ranger, N., Hallegratte, S., Corfee-Morlot, J., Herweijer, C., & Chateau, J. (2011). A global ranking of port cities with high exposure to climate extremes. *Climatic Change*, *104*(1), 89–111. <https://doi.org/10.1007/s10584-010-9977-4>
- Hay, C. C., Morrow, E., Kopp, R. E., & Mitrovica, J. X. (2013). Estimating the sources of global sea level rise with data assimilation techniques. *Proceedings of the National Academy of Sciences*, *110*(Supplement_1), 3692–3699. <https://doi.org/10.1073/pnas.1117683109>
- Jaroszweski, D., Chapman, L., & Petts, J. (2010). Assessing the potential impact of climate change on transportation: The need for an interdisciplinary approach. *Journal of Transport Geography*, *18*(2), 331–335. <https://doi.org/10.1016/j.jtrangeo.2009.07.005>
- Jongman, B., Winsemius, H. C., Aerts, J. C. J. H., Coughlan de Perez, E., van Aalst, M. K., Kron, W., & Ward, P. J. (2015). Declining vulnerability to river floods and the global benefits of adaptation. *Proceedings of the National Academy of Sciences*, *112*(18), E2271–E2280. <https://doi.org/10.1073/pnas.1414439112>
- Kellens, W., Terpstra, T., & De Maeyer, P. (2013). Perception and communication of flood risks: A systematic review of empirical research. *Risk Analysis*, *33*(1), 24–49. <https://doi.org/10.1111/j.1539-6924.2012.01844.x>
- Kopp, R. E., Horton, R. M., Little, C. M., Mitrovica, J. X., Oppenheimer, M., Rasmussen, D. J., ... Tebaldi, C. (2014). Probabilistic 21st and 22nd century sea-level projections at a global network of tide-gauge sites. *Earth's Future*, *2*(8), 383–406. <https://doi.org/10.1002/2014EF000239>
- Kopp, R. E., Mitrovica, J. X., Griffies, S. M., Yin, J., Hay, C. C., & Stouffer, R. J. (2010). The impact of Greenland melt on local sea levels: A partially coupled analysis of dynamic and static equilibrium effects in idealized water-hosing experiments: A letter. *Climatic Change*, *103*(3–4), 619–625. <https://doi.org/10.1007/s10584-010-9935-1>
- Kulp, S., & Strauss, B. H. (2017). Rapid escalation of coastal flood exposure in US municipalities from sea level rise. *Climatic Change*, *142*(3–4), 477–489. <https://doi.org/10.1007/s10584-017-1963-7>
- Leffler, K. E., & Jay, D. A. (2009). Enhancing tidal harmonic analysis: Robust (hybrid) solutions. *Continental Shelf Research*, *29*(1), 78–88. <https://doi.org/10.1016/j.csr.2008.04.011>
- Madadgar, S., & Moradkhani, H. (2014). Improved Bayesian multimodeling: Integration of copulas and Bayesian model averaging. *Water Resources Research*, *50*, 9586–9603. <https://doi.org/10.1002/2014WR015965>
- Maidl, E., & Buchecker, M. (2015). Raising risk preparedness by flood risk communication. *Natural Hazards and Earth System Sciences*, *15*(7), 1577–1595. <https://doi.org/10.5194/nhess-15-1577-2015>
- Moftakhari, H. R., AghaKouchak, A., Sanders, B. F., & Matthew, R. A. (2017). Cumulative hazard: The case of nuisance flooding. *Earth's Future*, *5*(2), 214–223. <https://doi.org/10.1002/2016EF000494>

- Moser, S. C., & Ekstrom, J. A. (2010). A framework to diagnose barriers to climate change adaptation. *Proceedings of the National Academy of Sciences*, 107(51), 22,026–22,031. <https://doi.org/10.1073/pnas.1007887107>
- Muis, S., Verlaan, M., Nicholls, R. J., Brown, S., Hinkel, J., Lincke, D., ... Ward, P. J. (2017). A comparison of two global datasets of extreme sea levels and resulting flood exposure. *Earth's Future*, 5(4), 379–392. <https://doi.org/10.1002/2016EF000430>
- Najafi, M. R., & Moradkhani, H. (2015). Multi-model ensemble analysis of runoff extremes for climate change impact assessments. *Journal of Hydrology*, 525, 352–361. <https://doi.org/10.1016/j.jhydrol.2015.03.045>
- Najafi, M. R., & Moradkhani, H. (2016). Ensemble combination of seasonal streamflow forecasts. *Journal of Hydrologic Engineering*, 21(1), 04015043. [https://doi.org/10.1061/\(ASCE\)HE.1943-5584.0001250](https://doi.org/10.1061/(ASCE)HE.1943-5584.0001250)
- Najafi, M. R., Moradkhani, H., & Jung, I. W. (2011). Assessing the uncertainties of hydrologic model selection in climate change impact studies. *Hydrological Processes*, 25(18), 2814–2826. <https://doi.org/10.1002/hyp.8043>
- Nicholls, R., Hanson, S., Herweijer, C., Patmore, N., Hallegatte, S., Corfee-Morlot, J., ... Muir-Wood, R. (2008). Ranking port cities with high exposure and vulnerability to climate extremes. <https://doi.org/10.1787/19970900>
- Nyborg, K., Anderies, J. M., Dannenberg, A., Lindahl, T., Schill, C., Schluter, M., ... de Zeeuw, A. (2016). Social norms as solutions. *Science*, 354(6308), 42–43. <https://doi.org/10.1126/science.aaf8317>
- O'Neill, A. C., Erikson, L. H., & Barnard, P. L. (2017). Downscaling wind and wavefields for 21st century coastal flood hazard projections in a region of complex terrain: Downscaling wind and wave fields. *Earth and Space Science*, 4(5), 314–334. <https://doi.org/10.1002/2016EA000193>
- Pfeffer, J., & Allemand, P. (2016). The key role of vertical land motions in coastal sea level variations: A global synthesis of multisatellite altimetry, tide gauge data and GPS measurements. *Earth and Planetary Science Letters*, 439, 39–47. <https://doi.org/10.1016/j.epsl.2016.01.027>
- Pielke, R., Prins, G., Rayner, S., & Sarewitz, D. (2007). Lifting the taboo on adaptation. *Nature*, 445(7128), 597–598. <https://doi.org/10.1038/445597a>
- Rattanaoch, W., Wang, Y., Chong, D., & Suwansawas, S. (2015). Adaptation strategies of transport infrastructures to global climate change. *Transport Policy*, 41, 159–166. <https://doi.org/10.1016/j.tranpol.2015.03.001>
- Ruggiero, P. (2013). Is the intensifying wave climate of the U.S. Pacific northwest increasing flooding and erosion risk faster than sea-level rise? *Journal of Waterway, Port, Coastal, and Ocean Engineering*, 139(2), 88–97. [https://doi.org/10.1061/\(ASCE\)WW.1943-5460.0000172](https://doi.org/10.1061/(ASCE)WW.1943-5460.0000172)
- Scavia, D., Field, J. C., Boesch, D. F., Buddemeier, R. W., Burkett, V., Cayan, D. R., ... Titus, J. G. (2002). Climate change impacts on U.S. coastal and marine ecosystems. *Estuaries*, 25(2), 149–164. <https://doi.org/10.1007/BF02691304>
- Schipper, E. L. F. (2009). Meeting at the crossroads?: Exploring the linkages between climate change adaptation and disaster risk reduction. *Climate and Development*, 1(1), 16–30. <https://doi.org/10.3763/cdev.2009.0004>
- Serafin, K. A., & Ruggiero, P. (2014). Simulating extreme total water levels using a time-dependent, extreme value approach. *Journal of Geophysical Research, Oceans*, 119(9), 6305–6329. <https://doi.org/10.1002/2014JC010093>
- Serafin, K. A., Ruggiero, P., & Stockdon, H. F. (2017). The relative contribution of waves, tides, and non-tidal residuals to extreme total water levels on US West Coast sandy beaches: REL CONT EXTREME TWL. *Geophysical Research Letters*, 44, 1839–1847. <https://doi.org/10.1002/2016GL071020>
- Shope, J. B., Storlazzi, C. D., Erikson, L. H., & Hegermiller, C. A. (2016). Changes to extreme wave climates of islands within the Western Tropical Pacific throughout the 21st century under RCP 4.5 and RCP 8.5, with implications for island vulnerability and sustainability. *Global and Planetary Change*, 141, 25–38. <https://doi.org/10.1016/j.gloplacha.2016.03.009>
- Spiekermann, R., Kienberger, S., Norton, J., Briones, F., & Weichselgartner, J. (2015). The Disaster-Knowledge Matrix—Reframing and evaluating the knowledge challenges in disaster risk reduction. *International Journal of Disaster Risk Reduction*, 13, 96–108. <https://doi.org/10.1016/j.ijdrr.2015.05.002>
- Tebaldi, C., Strauss, B. H., & Zervas, C. E. (2012). Modelling sea level rise impacts on storm surges along US coasts. *Environmental Research Letters*, 7(1), 014032. <https://doi.org/10.1088/1748-9326/7/1/014032>
- Temmerman, S., Meire, P., Bouma, T. J., Herman, P. M. J., Ysebaert, T., & De Vriend, H. J. (2013). Ecosystem-based coastal defence in the face of global change. *Nature*, 504(7478), 79–83. <https://doi.org/10.1038/nature12859>
- Titus, J. (2002). *Does sea level rise matter to transportation along the Atlantic coast? Presented at the potential impacts of climate change on transportation*. Washington, DC: U.S. Department of Transportation. Retrieved from https://www.transportation.gov/sites/dot.gov/files/docs/titus_Sea_Level_Rise_Matter_Transportation_Atlantic_Coast.pdf
- United Nations (2013). Climate change impacts and adaptation for international transport networks (Expert Group Report No. ECE/TRANS/238) (p. 223). Geneva, Switzerland: United Nations Economic Commission for Europe. Retrieved from http://www.unece.org/fileadmin/DAM/trans/main/wpp5/publications/climate_change_2014.pdf
- Wahl, T., Haigh, I. D., Nicholls, R. J., Arns, A., Dangendorf, S., Hinkel, J., & Slangen, A. B. A. (2017). Understanding extreme sea levels for broad-scale coastal impact and adaptation analysis. *Nature Communications*, 8, 16075. <https://doi.org/10.1038/ncomms16075>
- Weaver, C. P., Moss, R. H., Ebi, K. L., Gleick, P. H., Stern, P. C., Tebaldi, C., ... Arvai, J. L. (2017). Reframing climate change assessments around risk: Recommendations for the US National Climate Assessment. *Environmental Research Letters*, 12(8), 080201. <https://doi.org/10.1088/1748-9326/aa7494>
- Webb, E. L., Friess, D. A., Krauss, K. W., Cahoon, D. R., Guntenspergen, G. R., & Phelps, J. (2013). A global standard for monitoring coastal wetland vulnerability to accelerated sea-level rise. *Nature Climate Change*, 3(5), 458–465. <https://doi.org/10.1038/nclimate1756>